Power System Modeling and Performance Evaluation of Series/ parallel-type Plug-in Hybrid Electric Vehicles

Kazuki OCHIAI[1], Yusuke WADA[1], Yushi KAMIYA[1], Yasuhiro DAISHO[1], Kenji MORITA[2]
[1]WASEDA University, 55S-704, 3-4-1 Ohkubo, Shinjuku Tokyo, JAPAN
[2]Japan Automobile Research Institute, JAPAN
kazuki_o@waseda.jp

***Abstract*-In this paper, a simulator was built to simulate a plug-in hybrid electric vehicle (PHEV) power system. Specifically, a model adopting a series/parallel hybrid system with a planetary gear mechanism was created. With this model, the impacts of the engine on/off control and drive distance on environmental performance were analyzed using a homologation driving schedule for Japan. It was proven that when providing PHEVs to the market it will be necessary to adjust the engine on/off control to suit the actual daily drive distance of users.**

I. INTRODUCTION

A plug-in hybrid electric vehicle (PHEV) incorporates an electric drive capability using charging from an external power grid into the configuration of a conventional hybrid electric vehicle (HEV). The resulting vehicle system achieves zero-emission performance over short distance driving equivalent to a pure electric vehicle. Because of this fact, development is firmly underway in Japan, the US, and Europe with rising expectations of early practical application. However, the environmental performance of a PHEV varies greatly according to the distance it is driven. Therefore, any decision about whether to bring a PHEV to market must be determined based on performance evaluation using actual driving conditions.

In the research described in this paper, a simulator was built to simulate a PHEV power system. Specifically, a model adopting a series/parallel hybrid system with a planetary gear mechanism was created. With CO2 emissions as an index, the impacts of the engine on/off control and drive distance on the environmental performance were analyzed using homologation driving schedules.

II. PHEV MODELING

A. *PHEV Modeling Overview*

By using the homologation driving schedules as inputs, a model was constructed that is capable of calculating time-based changes in engine/motor output, current/voltage/state of charge (SOC) of the battery, fuel consumption, CO_2 emissions, and the like. An outline of the model is shown in Fig. 1[1]. The simulation results presented in this paper were obtained using this PHEV model, which was created with MATLAB/Simulink.

B. *Driving Schedule*

In consideration of vehicle use conditions, a Japanese homologation driving schedule (JC08) was adopted. The relationship between speed and time of the schedule is shown in Fig. 2.

C. *Vehicle Specifications*

The specifications of the simulated vehicle are shown in Table I. The vehicle was a widely used regular five-person passenger car and the hybrid system was a series/parallel-type incorporating a planetary gear mechanism. The fuel consumption (g/kWh) of the engine used in the calculation is shown in Fig. 3. The engine operated on the operating curve shown as the dot-dash-line [2]. The motor efficiency map is shown in Fig. 4.

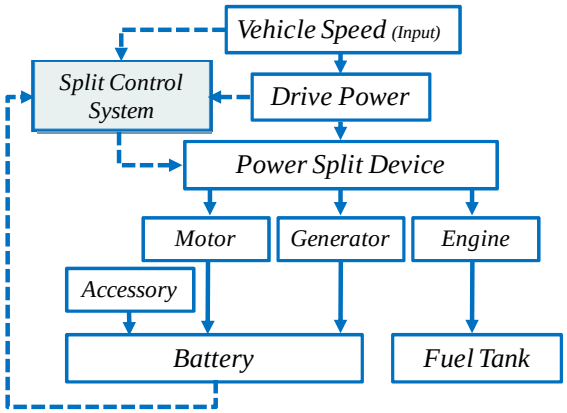

Fig. 1. Simulation Model

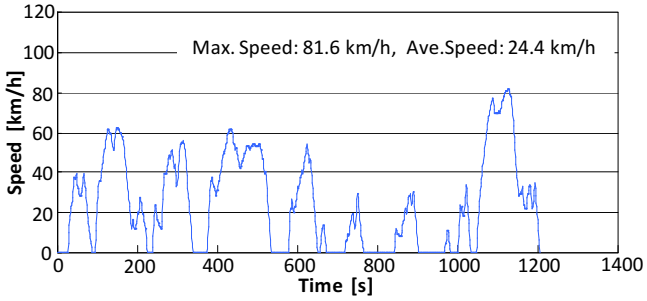

Fig. 2. Driving Schedule (JC08_JAPAN)

978-1-4244-8218-4/10/$26.00 ©2010 IEEE

TABLE I
VEHICLE SPECIFICATIONS

	Parameter	Set value
Weight	Curb Weight	1250 kg
	Equivalent rotational part mass	3.5% of Curb Weight
	Passenger mass	110 kg
Road load	Rolling resistance coefficient	0.01
	Air resistance coefficient	0.0343 N/(km/h)^2
Powertrain efficiency	Transmission efficiency	0.95
	Final gear efficiency	0.95
Engine	Refer to Fig. 3 (Displacement: 1.5 L) [2]	
Motor	Refer to Fig. 4 (Max power: 50 kW) [3]	
Generator	Max Torque	305 Nm
	Max Speed	12000 rpm
	Efficiency (Map)	from data base [4]
Battery system	Battery Weight	30 kg [5]
	Capacity	15 Ah
	Voltage	201.6 V
	Charge/Discharge efficiency	from data base [4]
	SOC range	90-30 %
Other	Braking method	Regenerative brake and Hydraulic brake

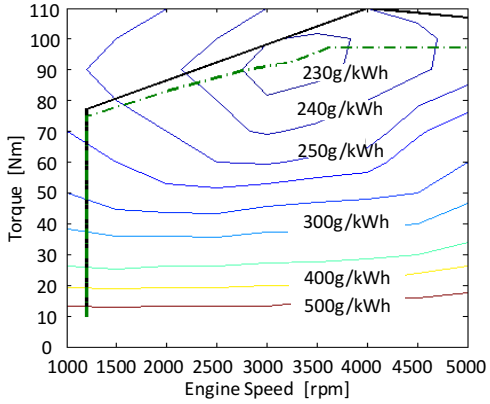

Fig. 3. Fuel consumption of the engine (g/kWh)

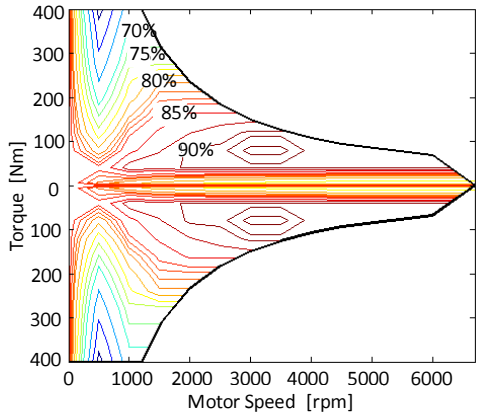

Fig. 4. Motor efficiency map

D. *Planetary Gear Modeling*

1. *Methods for Determining Planetary Gear Mechanism Rotation Speed and Torque*

A planetary gear model was used to split the power distribution. The generator was installed with a sun gear, the engine with a planetary gear carrier, and the motor with a ring gear, and all three mechanisms were connected. Their rotation speeds were connected in a linear fashion on a collinear diagram centering on the engine's rotation speed as shown in Fig. 5 [6]. The following relational equation expresses the rotation speed [7].

$$N_g = \left(1 + \frac{Z_m}{Z_g}\right) \times N_e - \left(\frac{Z_m}{Z_g}\right) \times N_m \quad (1)$$

where,
N: rotation speed
Z: number of gear teeth (Zg:30, Zm:78[8])
g: generator (sun gear)
e: engine (planetary gear)
m: motor (ring gear)

The ring gear was directly connected to the output shaft so that its rotation speed was determined by the vehicle speed. Generally in simulations, the engine power output is determined first and then the engine's rotation speed is calculated to achieve efficient driving. Having determined the engine power output and rotation speed, torque was obtained from Equation (2) and other torque calculations are shown in Equation (3), (4) [7].

$$T_e = \frac{P_{req}}{N_e} \quad (2)$$

$$T_g = \frac{Z_g}{Z_m + Z_g} \times T_e \quad (3)$$

$$T_m = T_d - \frac{Z_m}{Z_m + Z_g} \times T_e \quad (4)$$

where,
T: torque
d: drive shaft

2. *Reproduction of Cranking Phase*

The series/parallel-type HEV system described in this paper is not equipped with a starter. Instead the generator functions as the engine starter [9]. This research reproduced the cranking phase, which extends from the time that the engine start-up command is issued until the engine shifts to stable running, by modeling the planetary gear mechanism in detail.

In the cranking phase, as shown in Fig. 5, when the generator rotates in the negative direction it temporarily consumes the electrical power of the battery, but by reversing to rotate in the positive direction, it contributes to the rise in the engine speed. Consequently, if the amount of change in

the rotation speed of the generator is determined, then the rise in the engine speed can be expressed. The amount of change in the rotation speed of the generator is calculated using the equation of motion of the rotating body (Fig. 6).

An example of the calculation process is shown in Fig. 7. The figure shows the state immediately after the engine start-up command, when the generator takes on the role of the starter motor and enters the cranking phase, and then up to the point where the engine is running stably. The length of the cranking phase is held to within about 1 second. This period of time is equivalent to the lag that occurs from the engine start-up command until stable running.

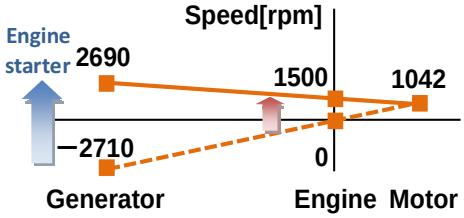

Fig. 5. Relationship between Rotation Speeds of Motor, Engine, and Generator(Vehicle speed:30km/h)

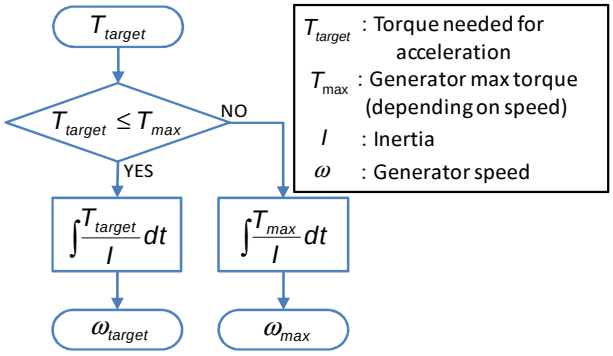

Fig. 6. Flow of Calculation for Generator Rotation Speed

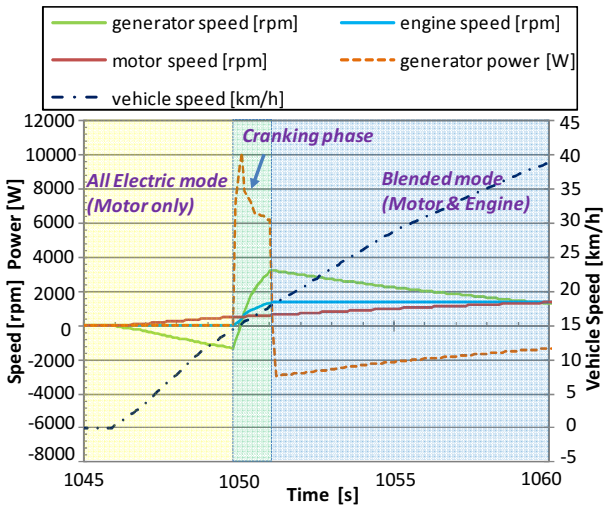

Fig. 7. Engine Start-up Lag

E. *Engine Modeling*

1. *Engine 'On' and 'Off' conditions*

Four patterns of engine on/off control (AER, Bld_20kW, Bld_15kW, and Bld_10kW) were established with the following three elements as triggers: the required drive power, the vehicle speed, and the battery SOC. The engine on/off command is determined by the following logic, and battery usage is possible within an SOC range of 90-30% according to this control logic.

a) The period from the time that the vehicle starts driving (SOC: 90%) until the battery reaches an SOC of 32.5% shall be charge depleting (CD) mode. If the SOC falls below 32.5% even one time, then it shall shift to charge sustaining (CS) mode [10].

b) When in the CD mode, if the conditions of 1) required drive power or 2) vehicle speed are satisfied, then the engine start-up command shall be issued (Table II).

c) After shifting into CS mode, the four control method patterns listed above shall no longer be used and instead the system shall switch over to a similar control method (high/low control) when it reaches the boundary at the SOC level of 32.5%. The threshold values used to make the individual engine on/off judgments under high and low control shall be as listed in Table III. By determining the output in this way, driving can be performed as if converging on the final SOC (32.5%) and it becomes possible to realize HEV driving using only a fixed SOC range.

d) In the case where none of the trigger conditions in Tables II and III are satisfied, a stop command shall be issued to the engine.

2. *Methods for Determining Engine Power Output*

In the case where an "on" judgment was issued (engine start-up command), the engine power output value is determined by the following equation. As shown in Equation (4), the engine power output value is controlled by the required drive power and battery SOC information.

However, the engine output ratio (α) in the equation is divided into two levels, one for output at high load and the other for all other output, with the boundary set at a drive torque of 50 Nm. The two levels of the engine output ratio are shown in Table IV.

$$P_{req} = \alpha \cdot P_{drive} + P_{add} \quad (4)$$

$$P_{add} = \beta \cdot (SOC_{target} - SOC) \quad (5)$$

provided that, $P_{add} \geq 0$

where,

P_{req}: power required for maximum engine output [W]

P_{drive}: power required for driving force [W]

P_{add}: power required for battery charging [W]

α: engine output ratio

β: power-charging coefficient [W]

SOC_{target}: target SOC 32.5% SOC: current SOC

TABLE II

ENGINE START-UP CONDITIONS (CD MODE)

Engine Control	CD mode: SOC: 90-32.5 %
AER*[1]	● Engine stop all time (only Motor Power)
Bld_20kW*[2]	● Drive Power: 20kW or over ■ Vehicle Speed: 55km/h or over
Bld_15kW*[2]	● Drive Power: 15kW or over ■ Vehicle Speed: 55km/h or over
Bld_10kW*[2]	● Drive Power: 15kW or over ■ Vehicle Speed: 55km/h or over

*1: All Electric Range Mode *2: Blended Mode

TABLE III

ENGINE START-UP CONDITIONS (CS MODE)

Hi (above 32.5 %)	Low (under 32.5 %)
● Drive Power: 10kW or over ■ Vehicle Speed: 55km/h or over	● Drive Power: 5kW or over ■ Vehicle Speed: 25km/h or over ◆ SOC: Under 30 %

TABLE IV

ENGINE OUTPUT RATIO

Driving Conditions	Engine Output Ratio
High Load (Drive Torque > 50 Nm)	95 % of Drive Power
General Load (Drive Torque ≦ 50 Nm)	55 % of Drive Power

III. VALIDATION OF THE MODEL

The model was validated by comparing its calculation results with actually measured values. The actually measured values are bench test data from a commercially-available HEV with the same specifications as the simulated vehicle. A European driving schedule (NEDC) was used for the measurements. The model discussed in this paper is for a PHEV. Therefore, in order to compare the results calculated from the model with the actually measured values of an HEV, the calculations were conducted after first changing the battery capacity to 6.5 Ah and the SOC range to 60±10%.

A comparison of the different engine speeds is shown in Fig. 8. Engine start-up timings, operating times, and engine speeds close to the actually measured values were obtained (solid line: real (actually measured) engine speed, broken line: simulated engine speed (calculated values), and dot-dash-line: driving schedule).

Next, the battery charge and discharge were compared (Fig. 9). It was found that the transitional battery charge and discharge power required for cranking at the time of engine start-up was expressed. (The discharge portions stand up like whiskers in the figure.) Through one cycle of NEDC, the obtained calculated results for both the engine speed and the battery charge and discharge power were generally close to the actually measured values.

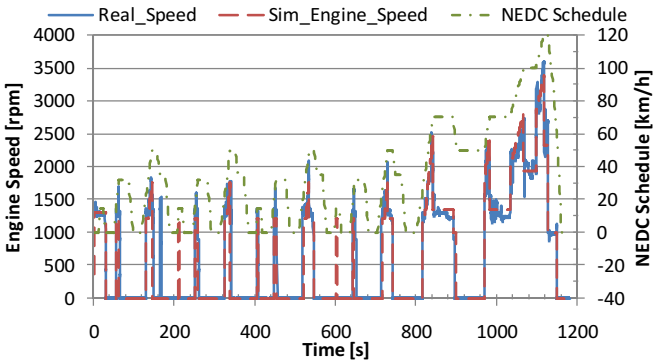

Fig. 8. Engine speed

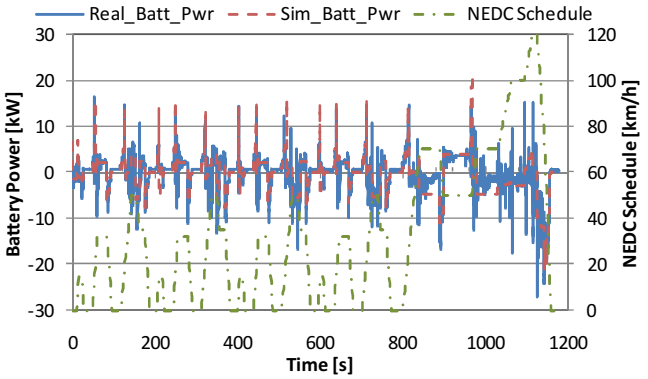

Fig. 9. Battery power

IV. PHEV ENVIRONMENTAL PERFORMANCE

The amount of CO_2 emissions was used as an index to assess environmental performance because this enables the amount of emissions to be determined not only during driving but also during electricity generation. In this paper, external charging energy refers to the energy amount required to recharge the battery to an SOC of 90% after driving. The equation below was used for calculations [11].

$$m_{CO2} = \frac{a_g \times V + \frac{a_e}{\eta_e} \times U}{d} \qquad (7)$$

m_{CO2}: CO_2 emissions [g-CO_2/km]
d: driving distance [km]
V: gasoline consumption [L]
U: electricity consumption [kWh]
(external battery charging output)
a_g: CO_2 emissions coefficient (gasoline) 2,360 g/L
a_e: CO_2 emissions coefficient (electricity) 555 g/kWh
η_e: power transmission efficiency 0.95
(Values take into account all the processes involved from the mined source material)

A. *Differences in Environmental Performance Depending on Engine On/Off Control*

The impact of the engine on/off control method on CO2 emissions was studied in the JC08 driving schedule. In this

study, a target drive distance *d* of 8.17 km was adopted to complete one cycle of JC08. The amount of CO2 emissions was determined in consideration of driving after a hot and cold start, respectively. The compound ratio of hot start to cold start is 0.75 to 0.25.

The calculation results are shown in Fig. 10. Relative to the base HEV, in all-electric range (AER), which involves driving throughout the entire cycle on battery power alone, a 23.2% reduction in CO2 was achieved.

B . Changes in Environmental Performance According to Drive Distance

PHEV are reported to be vehicles that produce remarkable differences in the amount of CO2 emissions depending on the drive distance. Therefore, this research sought to clarify the influence that the drive distance has on the amount of CO2 emissions by repeatedly driving the vehicle in the JC08 mode (Fig. 11).

The closer that the engine on/off control stayed to AER the more effective it was at reducing the amount of CO2 emissions over short distances. In contrast, it was found that at a drive distance of around 60 km and beyond, the effect of the engine control on the amount of CO2 emissions diminished. Furthermore, when the drive distance reached a range of around 130 km, the amount of emissions produced converged at around 75 g-CO2/km no matter which engine control was selected. The results showed that the dependence of the amount of CO2 emissions on the drive distance disappeared at this drive distance.

The following section compares the above results with the usage conditions of vehicles in Japan. In order to grasp these driving conditions it was necessary to find the single day distributions of drive distance throughout one year. To accomplish this, based on the method in reference [12], the data in reference [13] was approximated using a gamma function to derive the single day distributions of drive distance. The accumulation of these distributions is shown in Fig. 12. This research used a driver with an annual drive distance of around 10,000 km.

In Fig. 11 the amount of CO2 emissions in AER, Bld_20kW, and Bld_15kW control intersect at a drive distance of 24 km. It was found that when the section for a drive distance of 24 km is compared to Fig. 12, it accounts for around 50% of the number of days of vehicle operation. This means that if AER control was adopted for all of these days, it would be possible to drive a vehicle with CO2 emissions that are lower than those produced under Bld control for about half of the driving days during the year. It also shows the superiority of AER control from the standpoint of environmental performance.

Next, focusing on Bld control, the intersection point of all the Bld control lines can be seen at around a drive distance of 60 km. When the amount of CO2 emissions at this intersection point is compared to the base HEV, an effective reduction of about 7% can be seen. When this intersection point is compared to Fig. 12, it accounts for approximately 80% of the number of days of vehicle operation. Therefore, even if only Bld control was adopted, it would be possible to drive while maintaining an effective reduction in the amount of CO2 emissions of 7% or more in comparison to HEVs for approximately 80% of the days during the year. This ensures the superiority of PHEVs regardless of the type of engine control that is employed.

C. Selecting the Optimal Engine On/Off Control Method

As mentioned above, the type of engine on/off control that results in the minimum amount of CO2 emissions is different depending on the drive distance. This section examines how the engine on/off control should be selected by considering the reason for this.

Around a drive distance of 24 km the minimum amount of CO2 emissions changes from AER control to Bld_20kW. Therefore, at this point the amount of CO2 emissions in AER and Bld_20kW control were distinguished according to the origin of these emissions (Fig. 13). In order to grasp in detail the dependence of the amount of CO2 emissions on the drive distance, the real-time data was plotted (every 0.1 seconds).

The portion of CO2 emissions originating from the battery charging power is produced when the electricity is generated. Therefore, the amount of CO2 that is produced from battery charging power is the same in AER and Bld_20kW control. Consequently, the main cause of the difference in the amount of CO2 emissions according to the drive distance is the amount of CO2 produced from the gasoline. It is thought that the cause of this is that in CD mode the AER control provides the required drive power using only the motor, even when the engine is in an efficient driving region.

From the above results, it was found that selecting the engine on/off control that matches the driving range leads to optimal driving behavior. Therefore, it is thought that in order to allow a PHEV to exhibit its superior environmental performance to the maximum extent, the driver needs to be able to select the engine control method that corresponds to that day's drive distance, or a system should be adopted that automatically selects the engine control method when the day's destination is entered into the car navigation system.

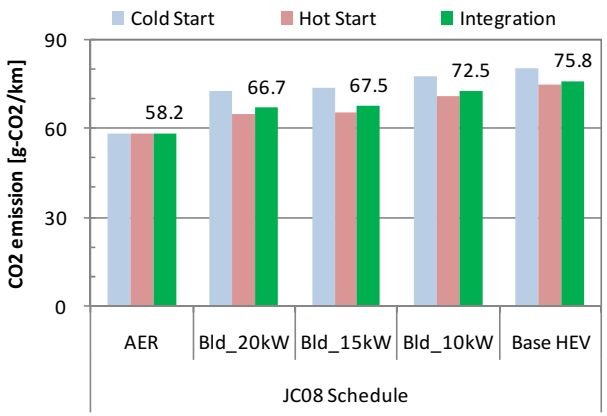

Fig. 10. CO_2 emissions depending on engine on/off Control

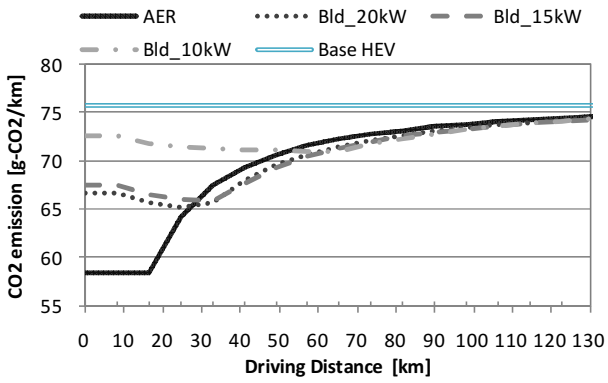

Fig. 11. CO_2 emissions (distance-dependent)

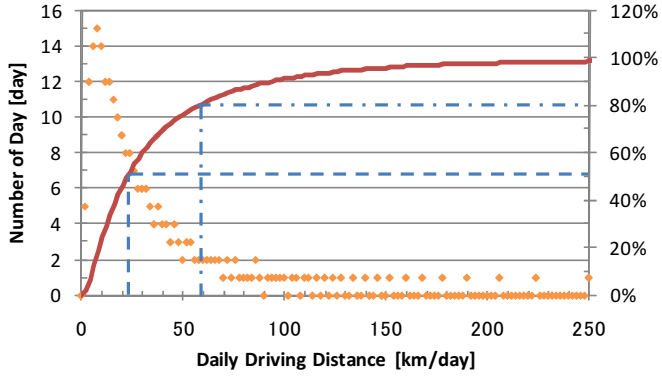

Fig. 12. Accumulative frequencies of daily driving distance for 1 year

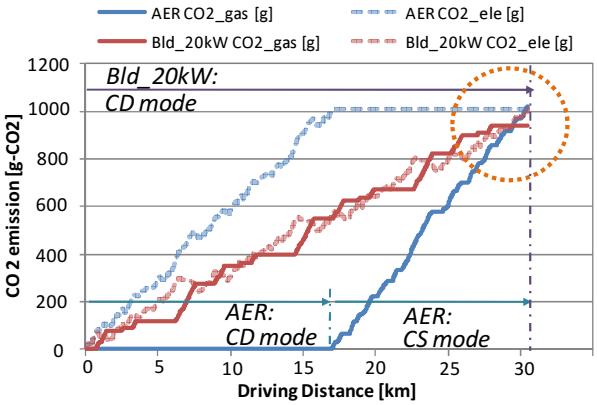

Fig. 13. CO2 Emissions According to Origin

V. Conclusions

a) A simulator was built simulating a PHEV power system and control methods. Specifically, a PHEV model was created adopting a series/parallel hybrid system with a planetary gear mechanism. Both battery power and the engine's rotation speed calculated by this model were almost equal to the measured data.

b) Using the simulator that was built, the influence of the engine on/off control method and drive distance on the amount of CO2 emissions from the PHEV was analyzed. When AER control was adopted for EV driving in all ranges during one cycle of the JC08 schedule, results were obtained that showed the amount of CO2 emissions were reduced by 23.2% compared to the base HEV.

In addition, when the vehicle was driven repeatedly in the JC08 schedule, it was found that at drive distances of 130 km and greater, no matter what engine control method was employed, the dependence on the drive distance became indiscernible. However, at drive distances of less than 130 km, it was found that the most advantageous engine control method was different depending on the drive distance. Therefore, it can be concluded that it is necessary to set the engine on/off control in accordance with the vehicle user's daily drive distance conditions.

Acknowledgments

This research was supported by New Energy and Industrial Technology Development Organization (NEDO). The authors would like to express their gratitude to the persons involved in the program.

References

[1] K. Muta, M. Yamazaki, and J. Tokeida, "Development of New-Generation Hybrid System THS II -Drastic Improvement of Power Performance and Fuel Economy," in *Proc. SAE World Congress*, Detroit, Michigan, USA, 2004.

[2] K. Naiki, N. Kawamoto, T. Kawai, T. Shikida, and K. Hayashi, "Development of New 1.8-Liter Engine for Hybrid Vehicles," in *Proc. JSAE Annual Congress(spring)*, Yokohama, Japan, 2009.

[3] ADVISOR2004, AVL List, 2004.

[4] Y. Wada, S. Shimada, W. Jibin, Y. Kamiya, Y. Daisho, and K. Morita, "Environmental performance evaluation of plug-in hybrid electric vehicles," *World Electric Vehicle Journal*, Vol. 3, pp.1-8, 2009.

[5] K. Morita, M. Akai, H. Hirose, "Development of Performance Test Procedure for Advanced Vehicle Batteries (First Report)," *JARI Research Journal*, vol.30, No.7 , pp.331-334, 2008.

[6] Y. Daisho, *Research of High Performance Electric Vehicle*, Sankaido , 2005.

[7] J. Park, J. Oh, Y. Park, and K. Lee, "Optimal Power Distribution Strategy for Series-Parallel Hybrid Electric Vehicles," in *Proc. IFOST*, Ulsan, Korea, 2006.

[8] S. Suzuki, K. Sera, et al., *Motor fan Illustrated-Toyota Prius Technology Details*, Sanei Shobo, 2009.

[9] Mojtaba Shams-Zahraei, and Abbas Z. Kouzani, "A Study on Plug-in Hybrid Electric Vehicles," in *Proc. IEEE TENCON 09*, Singapore, 2009.

[10] M. Duoba, R. W. Carlson, and J. Wu, "Test Procedure Development for "Blended Type" Plug-In Hybrid Vehicles," *SAE International Journal of Engines* , vol. 1, no. 1 , pp.359-371, 2009.

[11] Ministry of the Environment, Ministry of Economy, Trade and Industry, *Manual for Calculating and Reporting Greenhouse Gas Emission*, available at: http://www.env.go.jp/earth/ghg-santeikohyo.

[12] Ministry of Land, Infrastructure, Transport and Tourism, *Road Traffic Census*, JAPAN Society of Traffic Engineers, 1999.

[13] Y. Shinoda, H, Tanaka, A. Akisawa, and T. Kashiwagi, "Evaluation of the Plug-in Hybrid Electric Vehicle Considering Power Generation Best Mix," *IEEJ Trans.* , vol. 128, no. 6 , pp.827-835, 2008.